



**ARTICLE**

# Utilization of Recycled Concrete Powder in Cement Composite: Strength, Microstructure and Hydration Characteristics

Xi Chen<sup>1,2</sup>, Ying Li<sup>1,2,\*</sup>, Hualei Bai<sup>1,2</sup> and Liyuan Ma<sup>1,2</sup>

<sup>1</sup>School of Civil Engineering, Qinghai University, Xining, 810016, China

<sup>2</sup>Qinghai Provincial Key Laboratory of Energy Saving Building Materials and Engineering Safety, Xining, 810016, China

\*Corresponding Author: Ying Li. Email: liying.qh@163.com

Received: 16 December 2020 Accepted: 01 February 2021

## ABSTRACT

Recycled concrete powder (RCP) is used more and more in cement-based materials, but its influence on the hydration process is still unclear. Therefore, this paper studied the influence of recycled concrete powder (RCP) on the hydration process of cement and provides a theoretical basis for the hydration mechanism of cement composite materials. The hydration heat method was used to systematically analyze the thermal evolution process of cement paste with or without RCP. Hydration products were identified using X-ray diffraction (XRD) and thermal analysis (TG-DSC). The pore structure change of cement pastes was analyzed by mercury intrusion porosimetry (MIP) method. The mechanical properties of mortar were also evaluated. Four recycled concrete powder (RCP) dosages, such as 10%, 20%, 30% and 40% are considered. The results indicate that with the increase of RCP content, the hydration heat release rate and total heat release amount of paste decreased, but the second heat release peak of hydration reaction advanced; the proportion of harmful pores and more harmful pores increases, the total porosity and the most probable pore size also increase; the fluidity and mechanical strength of mortar decrease, but the crystal type of hydration products does not change. When the content of RCP is less than 20%, it has little effect on the mechanical strength of mortar. When fly ash and silica fume are mixed, the fluidity difference of mortar decreases, and when the content of fly ash is the highest, the fluidity of mortar is the highest, which is 15mm higher than that of the control group. When RCP content is 15%, fly ash and silica fume content is 15% (FA:SF = 3:2), the hydration heat of the clean pulp is the highest among all the compounding ratios, and the hydration reaction is the most complete; the proportion of harmless pores increased by 9.672%, the proportion of harmful pores and more harmful pores decreased, and the compactness of material structure increased; the compressive strength and flexural strength of mortar reached 50.6 MPa and 9 MPa respectively, both exceeding those of control mortar.

## KEYWORDS

Recycled concrete powder; hydration characteristics; microstructure; mechanical property

## 1 Introduction

Recent years, with the rapid development of urbanization, a large number of old buildings have been demolished and a lots of construction and demolition wastes (CDW) were generated also. For example, the annual output of CDW in China is about 1.8 billion tons, which has accounted for more than 1/3 of



the total amount of national waste, and the 40% of the total amount of CDW is waste concrete [1,2]. The main treatment method of CDW in China is dumping and landfilling, which has caused many environmental and social problems. Therefore, the recycling use of CDW have been a hot point for many scholars and experts. For example, coarse recycled aggregates and fine recycled aggregates, dust powder and waste fibers produced from CDW have been studied and partially applied in building engineering. The rational reuse of CDW not only can reduce the environmental pollution, but also alleviate the practical problem of increasing shortage of natural aggregate faced by concrete industry at present, benefiting society and environment.

Up to now, most of the researches are focused on coarse recycled aggregates (CRA) and fine recycled aggregates (FRA) in concrete. The addition of coarse recycled aggregates in concrete has been accepted, and it is even allowed to completely replace in some countries under particular situations [3]. While research on fine recycled aggregates is still relatively few, since some properties of recycled fine aggregate, such as workability, are more difficult to control due to its high porosity [4]. Then there is a scanty few related researches on the application of recycled concrete powder (RCP).

RCP is a kind of powder with a particle size below 150  $\mu\text{m}$  obtained by a mechanical pre-treatment (crushing, grinding and sieving) from construction and demolition wastes (CDW) [5,6]. CDW has higher reusability, lower cost and legal requirements and it is easy to obtain with high fineness and strong reactivity [7]. Furthermore, some studies have indicated that the proper replacement rate of CDW could not cause significant changes in mechanical properties [8,9]. Hence, the performance of RCP is worth studying. In addition, this kind of recycled powder contains a large number of fine particles, which will diffuse and float in the air if they are not collected and handled properly, causing air pollution and various diseases of the human body, e.g., lung cancer [10]. Now, Cement has been the most widely used building material of modern society due to its low cost and long durability. With the rapid development of economy, cities are expanding continuously, especially in developing countries. The consumption of cement will be increasing with the increase of infrastructure scale [11]. The mass consumption of cement has led to a significant reduction in non-renewable natural resources used as raw materials and a sharp increase in carbon dioxide emissions, which will aggravate environmental pollution [12]. Until now, numerous studies have shown that partially replacing the Ordinary Portland Cement (OPC) with one or more supplementary cementitious materials (SCM) with industrial solid wastes such as fly ash (FA), silica fume (SF), the construction and demolition wastes and so on is one of the most common ways to reduce cement energy consumption as well as protect the environment and achieve sustainable economic development [13,14]. Therefore, using an environmentally friendly method to reuse recycled micro-powder like fly ash as a supplementary cementitious material to produce green construction materials is a topic worthy of study, which contributes greatly to both public health and environmental sustainability.

Kima et al. [15] show that the particle size of RCP is larger than that of OPC, and the RCP mortar has low compressive strength and poor fluidity. The research results of Moon et al. [16,17] show that the mechanical properties of concrete are damaged by adding RCP, and the concrete performance can be improved by adding other admixtures or controlling the quality parameters of RCP. Jaroslav et al. [18–20] show that RCP contains some unhydrated cement particles, and the filling effect of micro-aggregate is remarkable, which can replace cement at low content. Kwon et al. [21] show that when RCP is used instead of cement, the overall performance can reach 80% even more of cement, and the carbon emission can be reduced by 46%. Rangel et al. [22] found that RCP particles have smaller average particle size, larger specific surface area and stronger water absorption, and suggested that RCP is feasible as an auxiliary cementing material. The research by Chen et al. [23] and Sun et al. [24] found that comparing the strength of samples containing recycled concrete powder with those without containing, the pozzolanic activity of RCP reached 70%, which indicates that RCP can be used as a substitute for cement. The research of Duan et al. [1,25] shows that when the content of RCP is less than 30%, it has a

positive influence on the mechanical properties of mortar. Liu et al. [26] found that RCP particles significantly reduced the fluidity of mortar and led to larger shrinkage.

Inspired by this, research exploring the application of RCP has attracted increasing interests. However, yet the progress has been made, the hydration mechanism of RCP needs to be further studied. As we all know, microstructure is the key to cement based material performance [27,28]. The hydration process of cement composites containing RCP is mainly divided into two steps. Firstly, cement reacts with water to form CH, C-S-H and Aft. Secondly, CH reacts with RCP and water to form C-S-H and C-A-H [29–31]. From the view of hydration, RCP motivates the hydration of cement through boundary nucleation and growth (BNG) effect. Such a process provides C-S-H and CH with places to precipitate and grow [32]. In addition, a porous structure of RCP accelerates cement mixes hydration, which leads to an initially higher hydration heat compared to cement [33]. This not only positively improves the mechanical properties of cement but also improves the hydration mechanism.

Hence, to respond to the need of systematic study on RCP and promote the application of RCP, this paper comprehensively investigated the hydration process and microstructure development of cement-recycled concrete powder binary system in combination with the mechanical properties of RCP cement-based materials. The curing period is from 3 days to 28 days. Different replacement rates of RCP (10, 20, 30, 40 wt%) are discussed. The heat evolution, hydration products type and morphology, pore structure of cement paste containing RCP were studied. The influence of RCP on cement and mortar strength was also studied then compared with OPC, the optimal dosage of RCP was obtained finally.

## 2 Experimental Program

### 2.1 Materials

The studied recycled concrete powders (RCP) were prepared with waste concrete in the laboratory. The waste concrete originated from the waste concrete beam in Xining railway traffic engineering project of Qinghai Province. The beam was made of CEM I 42.5 type Ordinary Portland cement (OPC), and the 28d compressive strength of the concrete beam was 32.4 MPa. The production of recycled concrete powders (RCP) consists of three steps. First, a waste concrete beam member was crushed into bricks by hand (Fig. 1a), then crushed by a jaw crusher and screened to obtain particles under 0.15 mm as recycled fines. Finally, the recycled fines were pulverized in a PM2L planetary ball mill for 30 min and selected as the studied recycled concrete powders (RCP) (Fig. 1b). Other materials used in these mixtures were CEM I 42.5 type Ordinary Portland cement (OPC), Class I grade fly ash (FA) and silica fume (SF).



**Figure 1:** Preparation of Recycled Concrete Powder (RCP)

The chemical composition and performance indicators of these materials are shown in Tabs. 1 and 2. The morphology of all particles are shown in Fig. 2. The particle size distribution curves of all particles are shown in Fig. 3 and Tab. 3. From the results, it can be seen that RCP and FA are much coarser than OPC and SF is

much finer than OPC. The mineral compounds of particles are shown in Fig. 4. It can be seen that the main chemical compositions of RCP are similar to that of OPC, including CaO, SiO<sub>2</sub>, Al<sub>2</sub>O<sub>3</sub>, Fe<sub>2</sub>O<sub>3</sub> and CO<sub>2</sub>, which account for more than 80% of the total components content of RCP. In addition, the total content of CaO, SiO<sub>2</sub>, Al<sub>2</sub>O<sub>3</sub> and Fe<sub>2</sub>O<sub>3</sub> accounts for more than 60% of all chemical components content of RCP. In RCP, CaO content is less than OPC, while SiO<sub>2</sub> content is higher than OPC and FA. This will help RCP play a pozzolanic role in cement hydration process. ISO standard sand was applied for mortar samples.

**Table 1:** Chemical composition of materials (%)

Materials	CaO	SiO <sub>2</sub>	Al <sub>2</sub> O <sub>3</sub>	Fe <sub>2</sub> O <sub>3</sub>	SO <sub>3</sub>	MgO	K <sub>2</sub> O	Na <sub>2</sub> O	TiO <sub>2</sub>	CO <sub>2</sub>
OPC	40.4	19.8	7.67	2.66	2.31	2.06	0.97	0.54	0.37	12.7
RCP	29.1	27.8	6.70	2.73	1.11	4.49	1.09	0.56	0.34	25.7
FA	1.27	21.5	15.20	1.36	0.24	0.40	0.68	0.4	0.41	58.3
SF	0.44	97.3	0.40	0.07	0.23	0.44	0.74	—	—	—

**Table 2:** Physical properties of materials

Materials	Bulk density (Kg/m <sup>3</sup> )	Apparent density (Kg/m <sup>3</sup> )	Specific surface area (m <sup>2</sup> /Kg)
OPC	1056	2978	493
RCP	856	2355	467
FA	1245	1919	438
SF	1560	2610	226

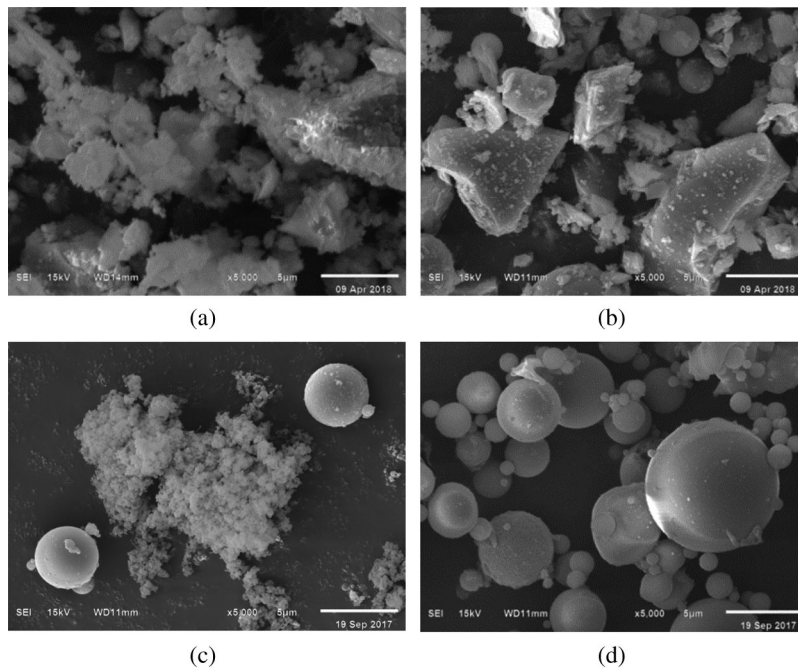


**Figure 2:** SEM images of materials  $\times 5000$ . (a) OPC, (b) RCP, (c) FA and (d) SF

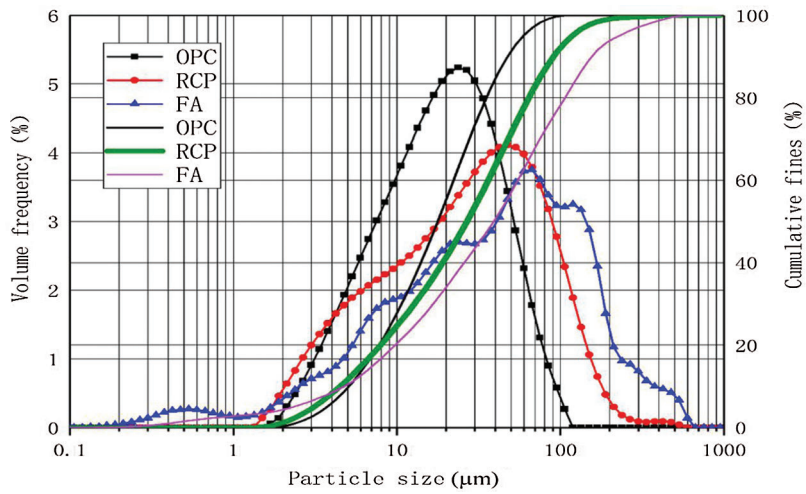


**Figure 3:** Particle size distributions of the component

**Table 3:** Particle size distributions of silica fume (SF) particles

Particle size distributions (µm)	<20	<50	Average grain diameter (µm)
SF(%)	100	100	0.82

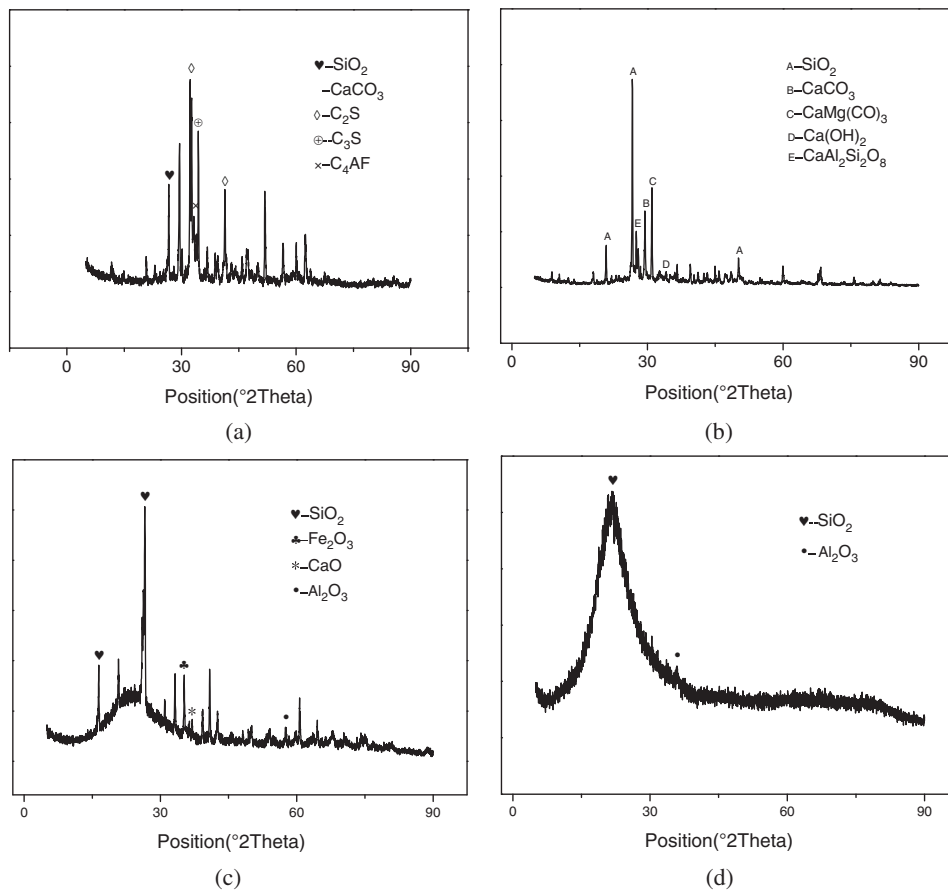


**Figure 4:** Mineral compounds of particles. (a) OPC, (b) RCP, (c) FA and (d) SF

## 2.2 Sample Preparation

The mix proportion of specimens is given in [Tabs. 4–7](#). [Tabs. 4 and 5](#) show the mix proportion of pastes. [Tabs. 6 and 7](#) show the mixture ratios of mortars. For all mixes, the type was OPC blended with RCP which were used to replace 0%, 10%, 20%, 30% or 40% of OPC respectively. In [Tabs. 4 and 6](#), the cement was partially replaced by 0%, 10%, 20%, 30% and 40% of RCP by weight, respectively. In [Tabs. 5 and 7](#), for improving the utilization rate of recycled fine powder the dosages of RCP were 30% partially replacement of OPC, FA and SF replaced RCP with a certain ratio as well. Each specimen was marked with a code, e.g., J1 and S1 represented 10% replacement of OPC by RCP. The reference samples are represented as J0 and S0. The paste specimens were stirred in a mixer with a mixing time of two minutes, then were modelled in rectangular moulds (20 mm \* 20 mm \* 20 mm) in their fresh states. For the mortar specimens, standard sand with particle sizes ranging from 0.5 mm to 1 mm was used as the aggregate. The mortar specimens were manufactured into cubes with a size of 40 \* 40 \* 160 according to the Chinese National Standard GB/T17671-1999 [26]. All demoulded specimens were kept in a curing room (at 20 ± 2°C, 95% RH) until the certain test age (3, 7 and 28 days). Absolute ethanol was used to stop the hydration reaction.

**Table 4:** Mix proportion of pastes

No.	Replacement rate (%)	W/C	OPC (g)	RCP (g)	FA (g)	SF (g)	Water (ml)
J0	0	0.45	455	0	0	0	205
J1	10	0.45	410	46	0	0	205
J2	20	0.45	364	91	0	0	205
J3	30	0.45	319	137	0	0	205
J4	40	0.45	273	182	0	0	205

**Table 5:** Mix proportion of pastes

No.	Replacement rate (%)	W/C	RCP (%)	FA+SF (%)	FA:SF	OPC (g)	RCP (g)	FA (g)	SF (g)	Water (ml)
F11	30	0.45	21	9	3:2	318.5	95.55	24.57	16.38	205
F12	30	0.45	15	15	3:2	318.5	68.25	40.95	27.3	205
F21	30	0.45	21	9	4:1	318.5	95.55	32.76	8.19	205
F22	30	0.45	15	15	4:1	318.5	68.25	54.6	13.65	205

**Table 6:** Mix ratios of mortars

No.	Replacement rate (%)	W/C	OPC (g)	RCP (g)	Sand (g)	Water (ml)
S0	0	0.5	450	0	1350	225
S1	10	0.5	405	45	1350	225
S2	20	0.5	360	90	1350	225
S3	30	0.5	315	135	1350	225
S4	40	0.5	270	180	1350	225

**Table 7:** Mix ratios of mortars

No.	Replacement rate (%)	W/C	RCP (%)	FA+SF (%)	FA:SF	OPC (g)	RCP (g)	FA (g)	SF (g)	Water (ml)
FS11	30	0.45	21	9	3:2	315	94.5	24.3	16.2	225
FS12	30	0.45	15	15	3:2	315	67.5	40.5	27	225
FS21	30	0.45	21	9	4:1	315	94.5	32.4	8.1	225
FS22	30	0.45	15	15	4:1	315	67.5	54	13.5	225

### 2.3 Testing Methods

Paste samples were used for setting time, hydration heat evolution, thermal analysis, hydration product type and pore structure tests. Mortar samples were tested for fluidity, compressive strength and flexural strength.

The setting time of all series of pastes was tested according to the Chinese standard GB/T 1346-2001 [34]. The fluidity of all series of mortars were tested according to the Chinese standard GB/T 2419-2005 [35]. An accurate conduction calorimeter (I-Cal 4000HPC, USA), with a working temperature of  $20 \pm 0.2^\circ\text{C}$ , was used to determine the change of hydration heat flow. Firstly, put the weighed material into the instrument and cover the instrument for preheating. After preheating for 2 h, take out the raw materials and stir them evenly, and put them into the hole inside the instrument again, and cover the instrument. The heat flow was recorded every 24 s until 72 h had passed. The hydration products were quantified and identified by thermogravimetry (TG)- differential scanning calorimetry (DSC) method.

Using the TG–DSC instrument at a controlled temperature, measure the mass change of cement paste as well as the energy difference between input cement paste and reference material. Nitrogen gas was employed as a protective gas to prevent carbonation in the heating process. During the test, samples were heated from room temperature to  $1000^\circ\text{C}$  at a heating rate of  $10^\circ\text{C}/\text{min}$ . The pore structures of pastes cured for 3, 7, and 28 days were characterized by mercury intrusion porosimetry (MIP). After reaching the required curing ages, the specimens were soaked in ethanol for one week to stop the hydration reaction. After the paste samples were taken out of the absolute alcohol, they were crushed into small particles with a diameter of approximately 2.36 mm and were oven dried in a vacuum at  $80^\circ\text{C}$  for 6 h. Experiments were carried out using an automatic mercury porosimetry (Autopore IV 9500), whose testing range of pore diameters was 0.007 to 144  $\mu\text{m}$ . MIP test consists of low pressure test and high pressure test. Firstly, put the weighed sample (about 2 g) into the dilatometer, and coat the upper surface of the glass tube with special glue for sealing. Then put the plastic sleeve on the dilatometer and put it into the low-pressure chamber for low-pressure test. After the low pressure test is completed, put the dilatometer into the high pressure chamber for high pressure test. After the test is completed, the data are exported for analysis. Crystallized phases of hydrated cement pastes were measured using an X-ray diffractometer (D/Max 2500PC, Japan). The acquisition range for each sample was  $5\text{--}70^\circ(2\theta)$ . Compressive and flexural strength tests were performed on samples with a loading rate of 0.3 kN/s after 3, 7 and 28 days of hydration. According to the Chinese standard GB/T 17671-1999 [36], each resultant value of compressive or flexural strength was an average calculated from several tests. When carrying out a strength test, the side perpendicular to the cube forming surface should be selected as the compression surface.

## 3 Result and Discussion

### 3.1 Setting Time Test Results

The setting time of all cement pastes studied is presented in Fig. 5. It indicates that both the initial and final setting time of cement pastes tended to be longer when RCP content increased. When the RCP content increased from 0 to 10%, the initial setting time of the cement paste decreased while the final setting time did

not change significantly. The setting time of the cement pastes was prolonged when the RCP content was higher than 10%. When FA and SF were added to RCP pastes, the setting time was significantly reduced. This may be attributed to the fact that the addition of FA and SF can promote the hydration of cement and make it form many flocculent CSH gels, thus losing plasticity and greatly shortening setting time [37].

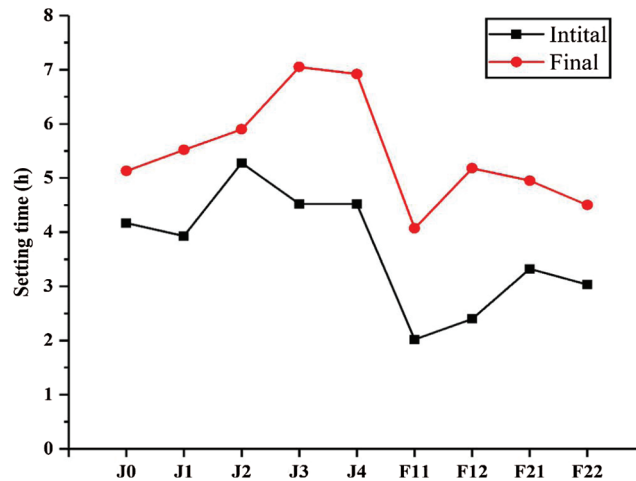


**Figure 5:** Setting time of cement pastes

### 3.2 Fluidity Test Results

As shown in Fig. 6, the fluidity of the control group S0 is 205 mm. Compared with the S0, the fluidity of samples doped only with RCP decreased significantly with the increase of the content of RCP. The reason for this result is that the recycled micropowder is porous, which leads to strong hygroscopicity [38]. It is obvious to find that RCP has a larger surface area compared to FA (Tab. 2) and the sample S3 with RCP is looser than the control sample S0 (Fig. 7), therefore, increasing the dosage of RCP naturally brings about a decrease in fluidity. However, it is interesting to note that the fluidity difference of samples decrease when mixed with composite RCP. Especially when the dosage of fly ash reaches the highest value (FS22), the fluidity also reaches the highest value (204 mm), which is similar to that of the control group. This may be due to the ball-bearing effect of FA. The fly ash particles act as a “ball bearing” in the mortar, reducing the internal friction between fly ash and other particles, and at the same time reducing the agglomeration and breaking of flocs, releasing locked water [39].

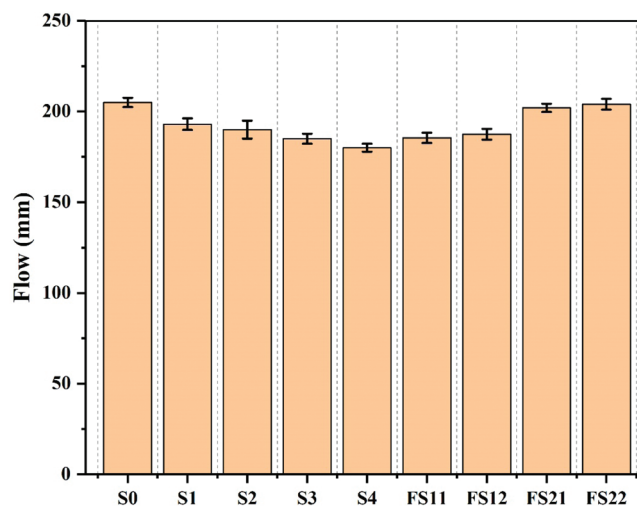


**Figure 6:** Flow of cement mortar adding RCP

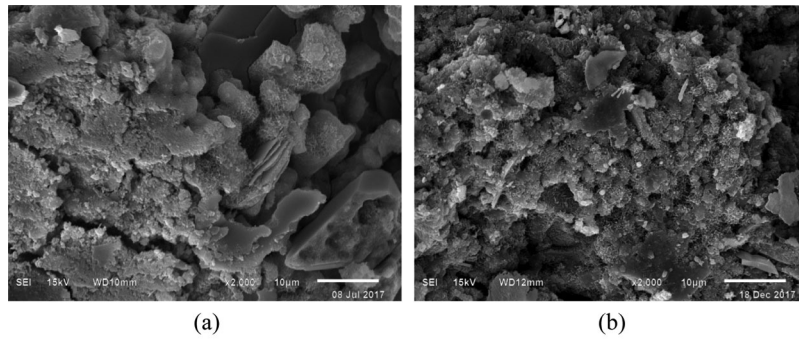


Figure 7: SEM images of pastes  $\times 2000$ . (a) S0-28d and (b) S3-28d

### 3.3 Mechanical Property

The results of compressive and flexural strength tests are presented in Figs. 8a–8d. The influence of RCP on the compressive strength of mortars is found to be similar to that on flexural strength.

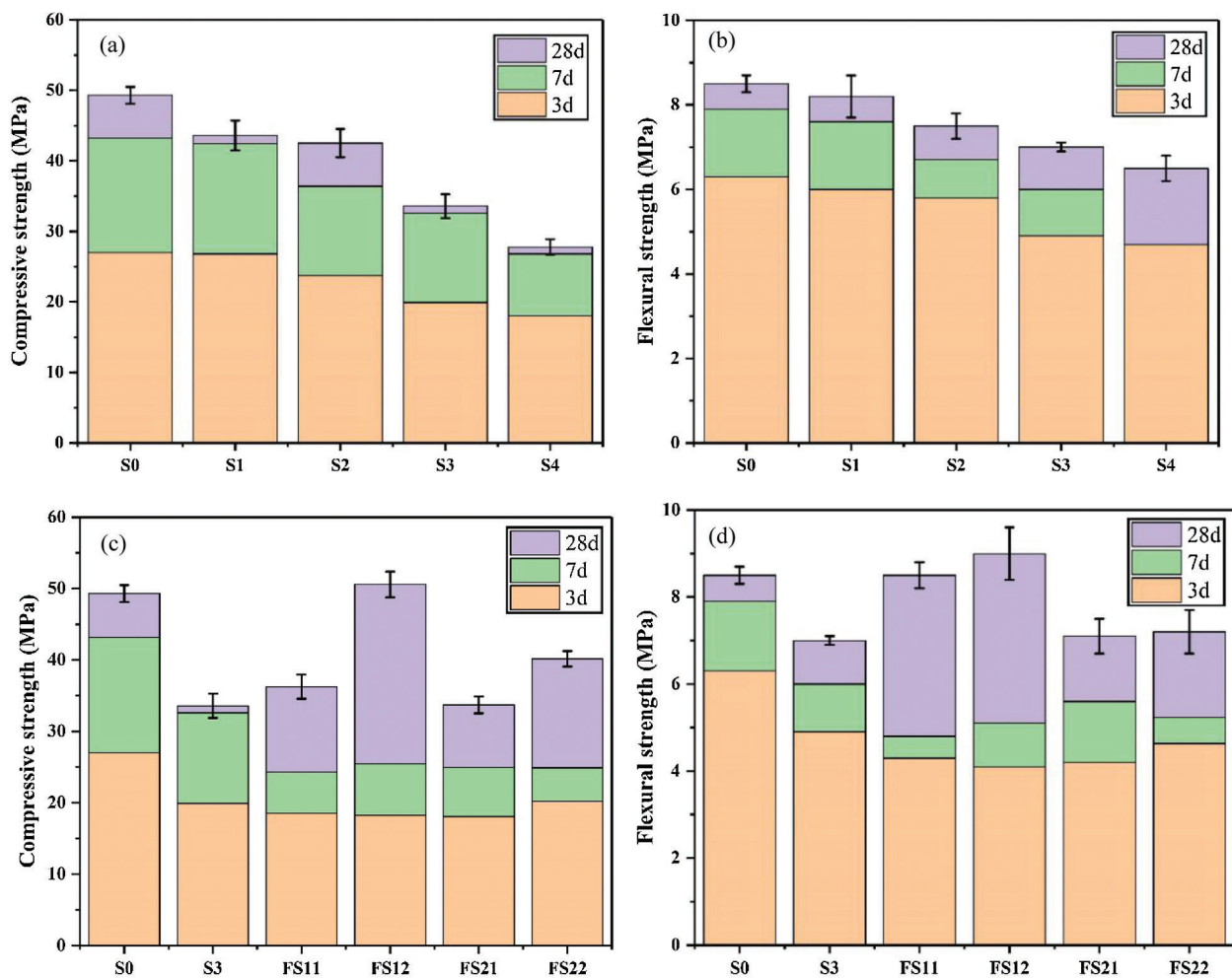


Figure 8: Compressive strength and flexural strength of mortars with and without RCP. (a) Compressive strength of mortars, (b) Flexural strength of mortars, (c) Compressive strength of mortars and (d) Flexural strength of mortars

Figs. 8a and 8b show that the compressive and flexural strength of mortars dropped noticeably as the RCP dosage increased at every age. When the dosage is 10%, the compressive strength of RCP mortar is similar to that of the reference mortar at 3 days and 7 days, while it is slightly lower at 28 days. When the dosage is 20%, the compressive and flexural strength of RCP mortar has a small decrease, but it still reaches more than 80% of the reference mortars. When the dosage was 30% and 40%, the strength of RCP mortar both decreases significantly compared with the reference mortar. This may attribute to the high content of CaO and SiO<sub>2</sub> in RCP, which has more active components. These active oxides reacted to form the C-S-H gel, which leads to more complete hydration and increased the strength of the concrete (see Tab. 1 and the TG–DSC analysis) [40,41]. Secondly, RCP had lots of fine powders (particles with sizes under 10 μm), and these ultrafine powders filled the pores in the cement paste, improving the pore structure and strength of the mortar (see analysis of the MIP test) [42]. However, when the RCP content is higher than 20%, the mortars cannot be bonded together to form a stress structure, resulting in slightly lower strength, due to the excessive content of fine powder in the RCP, or the hydration of the powder itself is very limited.

Figs. 8c and 8d show the comparison of compressive strength and flexural strength of the mortars mixed with blended RCP with the reference mortar. It can be noticed that compared with the reference mortar, the strength growth of mortars mixed with blended RCP in 3 days and 7 days is lower, while the strength growth in 28 days is larger, which is just opposite to the reference mortar. This indicates that blended RCP reduces the early strength of mortars, but improves the long-term strength of that. The main reason for this phenomenon is that in the early hydration stage, FA and SF mainly play the role of micro-aggregate filling in cement paste, while in the later hydration stage, the pozzolanic reaction of fly ash increases, which leads to more complete hydration and enhances the compactness of mortar microstructure, thus making the long-term strength increase greatly [1,43,44]. At 28 days, the strength of most composite mortars is lower than that of the reference mortar, however, the compressive strength and flexural strength of FS12 both surpassed that of S0, reaching 50.6 MPa and 9 MPa respectively. It means that adding FA and SF particles into RCP mortar in proper proportion is beneficial to improve the flexural strength and enhancing the crack resistance. The research of Li et al. also reached a similar conclusion [45].

### 3.4 Hydration Heat Test Results

It can be seen from Figs. 9 and 10 that there are three peaks in the hydration process, the first peak is the reaction of aluminate with water and sulfate in the early stage of induction, forming a gel-like material (ettringite) around the cement particles, releasing a lot of heat; the second peak is the formation of fibrous calcium silicate hydrate (C-S-H) gel and crystalline calcium hydroxide (CH) in acceleration period, with obvious thermal evolution; the third peak is that the interaction of C-S-H gel and crystalline CH with the remaining water and undissolved cement particles during the deceleration period slows the C<sub>2</sub>S reaction, thereby reducing the heat of hydration. The sulfate begins to be consumed, so the remaining aluminate reacts with ettringite to form monosulfate [40].

The results of hydration heat of RCP, FA, SF pastes and OPC paste are compared in Figs. 9a and 9b. The dosages of RCP, FA, SF are all considered as 10%. It can be seen from Fig. 7a that the order of hydration heat rates is OPC-100% > RCP-10% > FA-10% > SF-10% at 72 h. Fig. 7b shows that RCP paste has the highest total hydration heat among all pastes from 0 to 72 h. This indicates that the hydration reaction of RCP is more complete compared with FA and SF. RCP, with a high initial heat rate, produces more hydration products, so it is more suitable to be used as supplementary cementitious material.

Figs. 9c and 9d show the comparison of pastes doped with RCP and OPC. It can be seen that the order of heat release rate and total hydration heat both decrease with the increase of RCP dosage, and are both lower than OPC. The highest peak of hydration heat release rate occurs three times at 10% of single-mixed RCP, the first peak can be ignored, because it indicates the beginning of the hydration reaction of aluminate (C<sub>3</sub>A), the

main product is ettringite (AFt). The higher the content of RCP is, the earlier the peak of the secondary hydration reaction will be. This indicates RCP accelerates the cement hydration. This indicates that RCP with fine particles accelerates cement hydration, which is consistent with the research results of Jiang et al. [44]. The reason may be the dilution of cement, or the increase of nucleation sites caused by hydration reaction [46]. Compared with cement, RCP reduces the content of gypsum and improves the reactivity of C<sub>3</sub>A, so that C<sub>3</sub>A can renew and accelerate hydration.

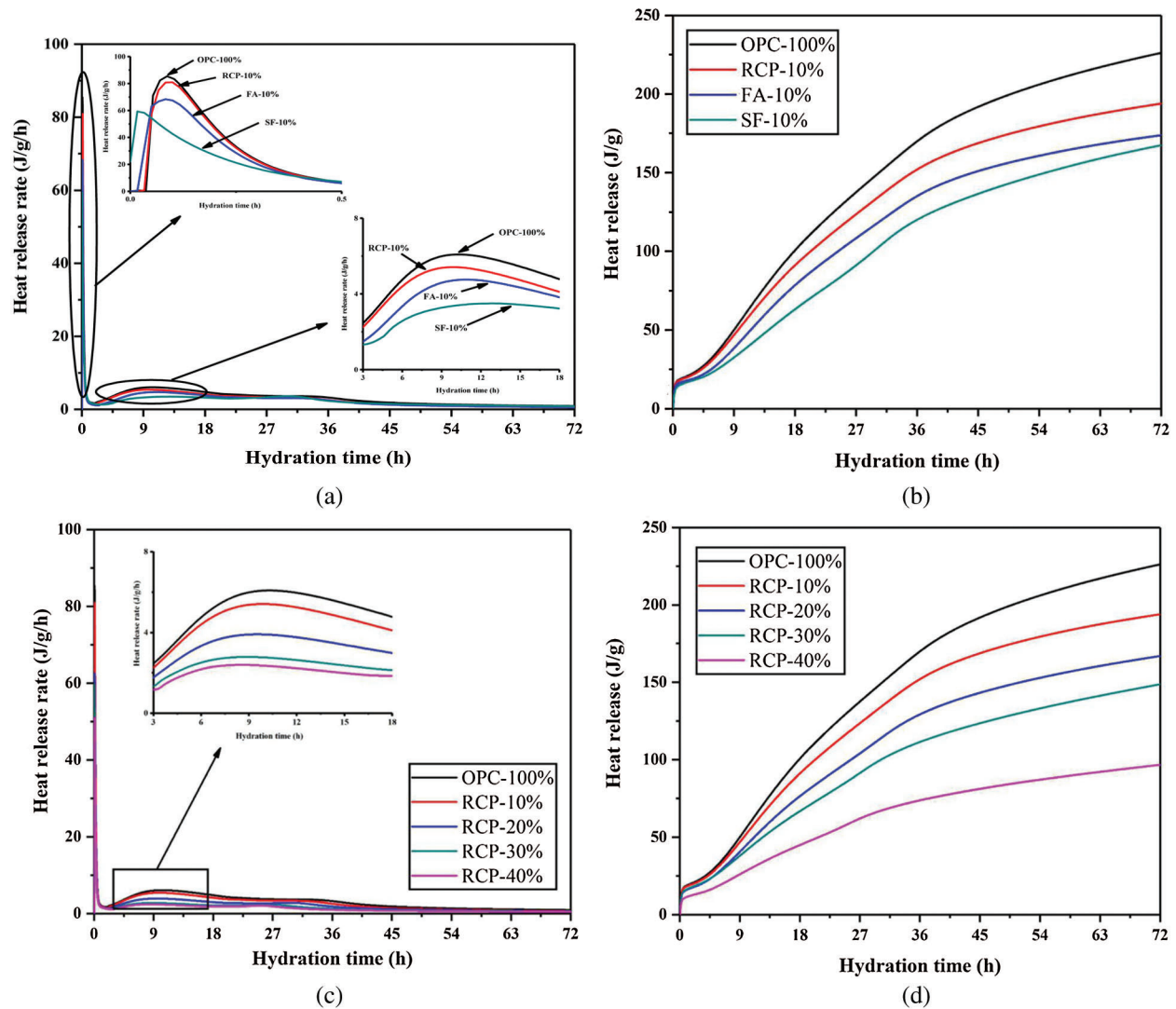


**Figure 9:** Heat evolution curves of samples. (a) The hydration rate in 72 h, (b) The cumulative hydration heat in 72 h, (c) The hydration rate in 72 h and (d) The cumulative hydration heat in 72 h

Figs. 10a and 10b show the comparison of OPC samples, RCP single-doped samples and composite RCP samples (the RCP replacement rate is 30%). It can be found that the hydration heat release rate is in the order of OPC-100% > RCP-F12 > RCP-F22 > RCP-F11 > RCP-F21 > RCP-30%; the total heat release is in the order of OPC-100% > RCP-30% > RCP-F12 > RCP-F22 > RCP-F11 > RCP-F21. This shows that when the dosage of RCP is 30%, the proportion of other mineral admixtures mixed with 50% release more heat than 30%, and when FA:SF = 3:2 also release more heat than FA:SF = 4:1. This shows

that under the same dosage of RCP, for composite RCP samples, the hydration reaction is more complete when the proportion of other mineral admixtures is 50% (FA:SF = 3:2). This indicates that FA increases the hydration reaction rate of cement to a certain extent due to its nucleation effect in the hydration reaction of the paste. Matos et al. found that the higher the pH of pore solution was, the stronger the reaction degree of  $C_3A$  was [47]. Because FA contains aluminates, which can undergo alkaline activation reaction in the process of cement hydration then promote cement hydration and generate inorganic polymer, thus making the mechanical properties of the material stronger. Tang et al. [48] also show that the cement mixture mixed with RCP and FA is helpful to improve the properties of cement composites.

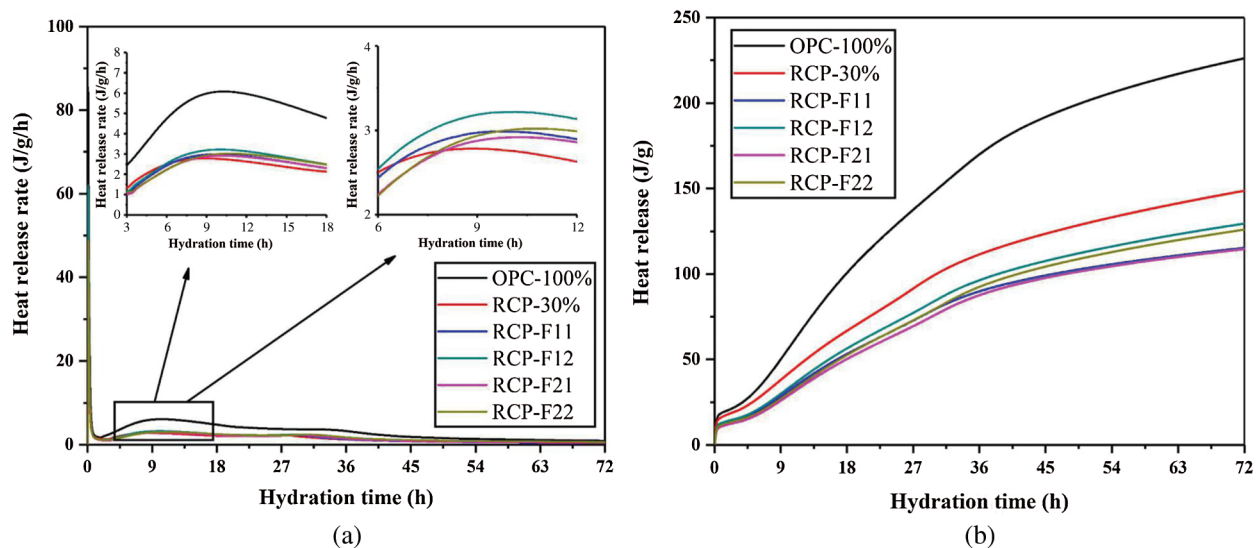


**Figure 10:** Heat evolution curves of samples. (a) The hydration rate in 72 h and (b) The cumulative hydration heat in 72 h

### 3.5 X-ray Diffraction Analyses

Figs. 11a and 11b illustrates the XRD pattern of cement pastes with curing time of 28 days. Comparing with OPC paste, there are no new hydration products generated for RCP pastes. The only difference is the diffraction peak intensity of portlandite (CH) and ettringite (Aft). Along with hydration process, the silicon dioxide ( $SiO_2$ ) and belite ( $C_2S$ ) from pastes was consumed and portlandite (CH) and ettringite (Aft) were produced with time. As can be seen from Fig. 11a, when RCP is doped alone, as the dosage increases, the contents of CH and Aft decrease. When the dosage of RCP is 10%, the content of CH and Aft is the highest, which is close to the control group, this shows that the hydration reaction is more complete. When the dosage of RCP is 20%, the content of  $C_2S$  is the highest leading to incomplete hydration reaction, which maybe because the hydration rate of  $C_2S$  is slower than that of  $C_3S$ . The Aft content in J0 is the highest, because the gypsum content in RCP is relatively small, so the formation of Aft phase is less [49].

From Fig. 11b, CH in the F12 sample increases slightly, but other crystalline compounds do not make much difference. Compared with J0, the intensity of CH diffraction peaks of other samples highly decreased, but that of  $C_2S$  and  $SiO_2$  are sharply enhanced. The consumption of CH can be attributed to the pozzolanic reaction of  $SiO_2$  from RCP composite paste [50–53]. This result means that the FA and SF particles in RCP composite paste can promote the formation of nucleation point, and with the rehydration of cementitious

materials, CH crystals decrease, and  $\text{CaCO}_3$  in the product fills the surface pores [54]. As observed in other studies, this accelerates the improvement of material mechanical properties [55–57].

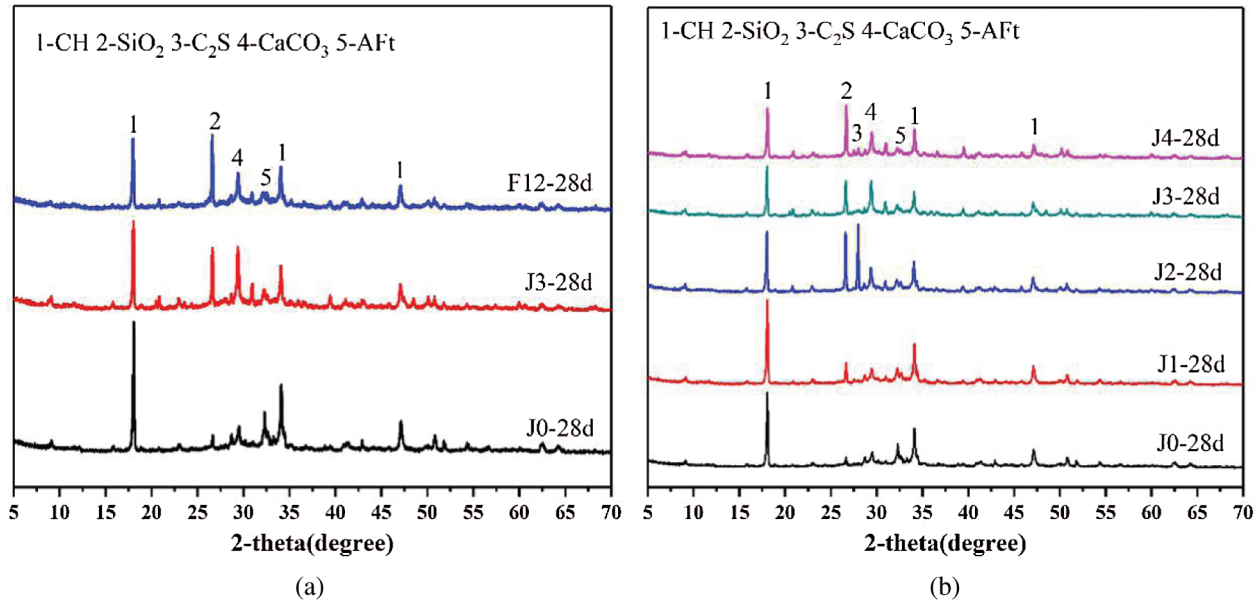


**Figure 11:** XRD pattern of hydration product. (a) Pastes with different RCP content and (b) Pastes with different RCP content

### 3.6 TG-DSC Test Results

For further analyzing the influence of RCP on the hydration of cement paste, the hydration products of hydrated cement pastes were used for characterization. Materials released during TG–DSC process was monitored by MS instrument, and test results are concluded in Tab. 8. The TG–DSC curves of cement paste without and with RCP or FA are given in Figs. 12a and 12b. The TG–DSC test was performed in nitrogen atmosphere. The first exothermic peak at 120°C is attributed to the water release behavior of CSH gel and AFt phase; the second peak at 450°C is attributed to the decomposition of calcium hydroxide(CH); and the peak at 700°C is attributed to the decomposition of calcium carbonate ( $\text{CaCO}_3$ ). In addition, it can be noticed from the figure that the quality has also changed accordingly. The chemical reaction equations that occur during the hydration of cement are [11,58].



**Table 8:** Relationship between temperature and release materials

Temperature/°C	Water	$\text{CO}_2$
120	×(Water released from CSH or Aft)	
450	×(Decomposition of CH)	
700		×(Decomposition of $\text{CaCO}_3$ )

At 450°C, cement pastes cured for 28 days (Fig. 12a) shows the order of mass loss is J0 (4.70%) > J1 (3.99%) > J2 (3.86%) > J3 (3.37%) > J4 (3.21%). This confirms that compared with the reference group, with the increase of RCP content, the generated CH content gradually decreases, which proves that RCP can promote the hydration of cement, and its nucleation provides sufficient nucleation sites for the formation of hydration products. From Fig. 10b, the order of mass loss is J0 (4.70%) > J3 (3.37%) > F12 (2.28%) at 450°C. This indicates that with the addition of FA and SF, the content of CH in the mixed paste decreases obviously, which is due to the enhancement of pozzolanic reaction of mixed paste, consuming more CH and producing C-S-H gel [59–61]. It is confirmed again that the pozzolanic effect of sample with composite RCP is stronger than that only with RCP.

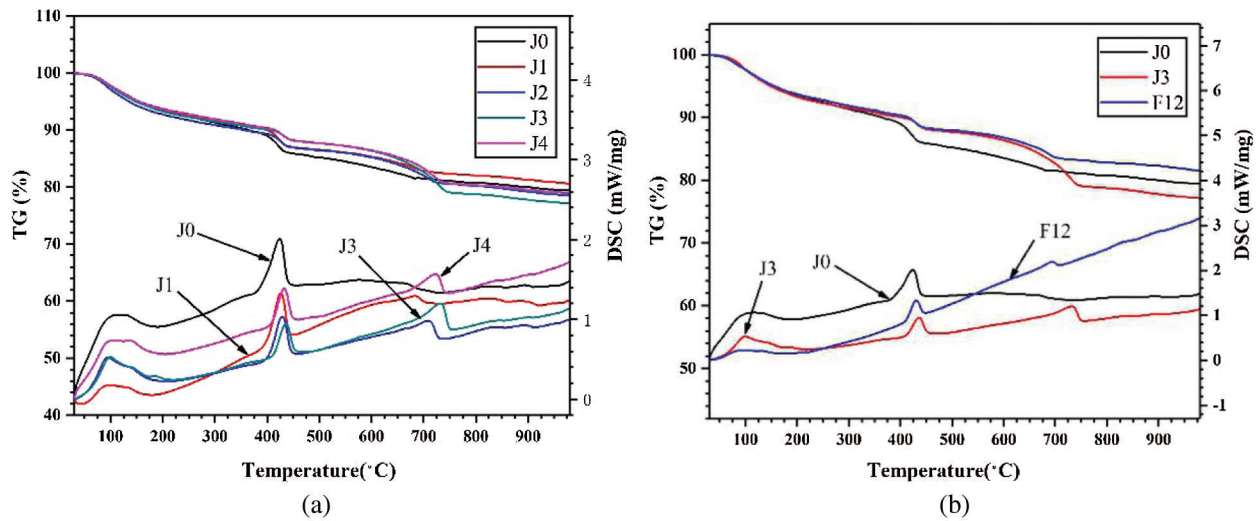


**Figure 12:** TG-DSC curve of cement pastes. (a) Pastes with different RCP content and (b) Pastes with different RCP content

### 3.7 Pore Structure Evolution

The results of the MIP analyses of the paste samples cured for 28 days are shown in Figs. 13a–13d. With reference to Academician Wu Zhongwei's division of concrete pores, those with a pore diameter of <20 nm are harmless pores (Zone I), 20–50 nm are less harmful pores (Zone II), 50–200 nm are harmful pores (Zone III), and > 200 nm are more harmful pores (Zone IV) [62]. Figs. 13a–13d indicate that with the incorporation of RCP in the pastes, the pore structures of the paste samples exhibited different changes. Fig. 11a shows that the most probable pores of the samples are all in the Zone III, at 28 days, the most probable pore size of each series ranges from small to large as follows: J3(95.389 nm) < J2(95.485 nm) < J1(95.529 nm) < J0 (95.559 nm) < J4(120.995 nm).

Figs. 13b and 14 show that the pore size distribution of samples is mainly distributed in harmful pores and more harmful pores. With the increase of RCP content, the content of harmful pores decreased, the content of harmful pores increased and the total pore volume increased. When the content of RCP is 40%, the more harmful pores become the pores with the highest content in pastes. However, when the content of RCP is 10%, compared with the control group, the content of harmful pores decreased by 4.338%, the content of more harmful pores increased by 4%, but the content of harmless pores increased by 1.653%. This indicates that the fineness of RCP is small, and that proper addition of RCP to pastes can refine the most possible pore size, make the hydration reaction more complete, produce more hydration products and transform harmful pores into harmless pores to form a denser pore structure [63–66]. While excessive RCP will cause the reduction of hydration products and weaken the refining effect of RCP. As a result, harmful pores and more harmful pores gradually increase, and RCP plays a completely opposite role.

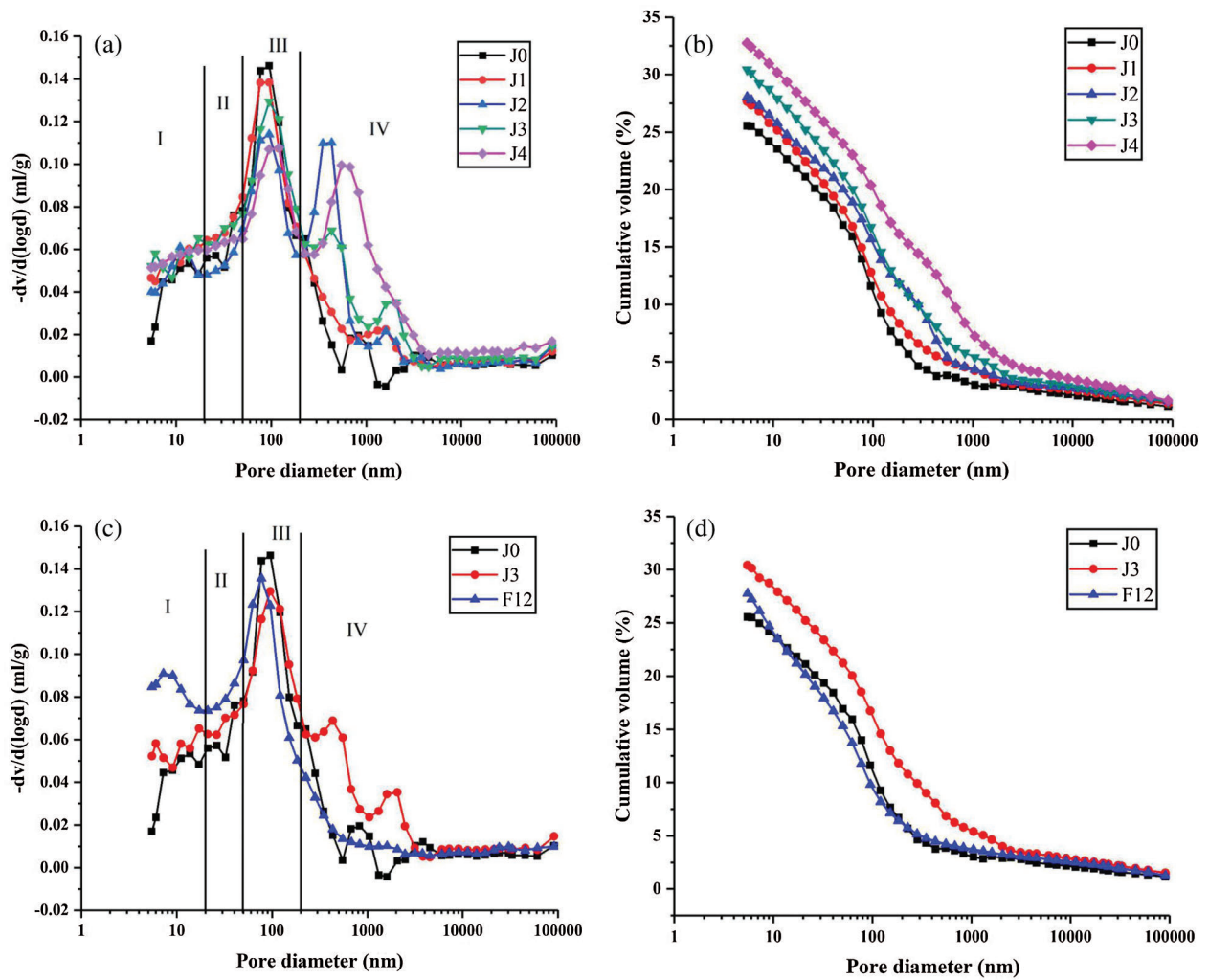


**Figure 13:** Pore size distribution of cement pastes at 28 d. (a) Differential pore size distribution of cement pastes, (b) Cumulative pore size distribution of cement pastes, (c) Differential pore size distribution of cement pastes and (d) Cumulative pore size distribution of cement pastes

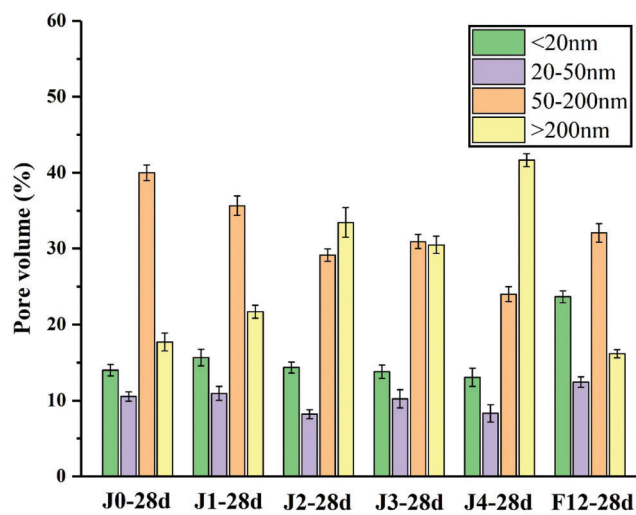


**Figure 14:** Pore volume distribution of Paste

Fig. 13c shows that the most probable pores of the samples are all in the Zone III, at 28 days, the most probable pore size of each series ranges from small to large as follows: F12(77.180 nm) < J3 (95.389 nm) < J0(95.559 nm). Figs. 13d and 14 show that when FA and SF are mixed, compared with J0, J3, F12 greatly increases the ratio of harmless pores and reduces the ratio of harmful pores and more harmful pores. The proportion of harmless pores in F12 increased by 9.672% compared with J0. The total pore volume of each series ranges from small to large as follows: J0 < F12 < J3. This indicates that adding a proper amount of FA and SF can significantly improve the pore structure of the RCP cement pastes at the same content, making the structure more dense and uniform, which should be mainly related to the morphology and filling effect of them [67,68]. This is consistent with the previous discussion results in this paper.

#### 4 Conclusions

In this paper, the influence of single and mixed RCP of different dosages on the performance of cement mortar and mortar is studied by means of hydration heat, TG-DSC and MIP, etc. Based on the above mentioned experimental results, the following conclusions can be drawn:

1. Compared with cement, RCP is much coarser and the content of  $\text{SiO}_2$  is higher. With the increase of RCP content, the fluidity of mortar decreased, and the setting time of paste increased. Adding FA and SF improved fluidity and shorten setting time.
2. With the increase of RCP content, the compressive strength and flexural strength of mortar at different ages decreased. When the dosage of RCP was less than 20%, the 28-day compressive strength and flexural strength of RCP mortar decreased slightly, reaching more than 80% of the control group. After FA and SF were added into RCP mortar, due to the physical filling and chemical action of active powder, the early strength of mortars decreased, but the later strength increased. When the content of RCP is 15%, the replacement rate of other mineral admixtures is 15% (FA:SF = 3:2), the compressive strength and flexural strength of mortar were the highest, reaching 50.6 MPa and 9 MPa respectively, which both exceeding those of the control group.
3. The analysis of hydration heat showed that with the addition of RCP shortened the induction period and reduced the heat release rate and the cumulative heat at 72 h, and was lower than that of the control group. When FA and SF were mixed in RCP pastes, the pozzolanic effect increased, and the heat release rate increased in 72 h. When the paste ratio is F12 (The RCP dosage is 15%, the substitution rate of other mineral admixtures is 15%, FA:SF = 3:2), the cumulative heat was the highest among the RCP samples mixed with FA and SF.
4. XRD and TG analysis showed that the addition of RCP did not change the crystal type of hydration products. With the increase of RCP dosage, the content of CH in the product decreased, and the hydration reaction degree decreased. When FA and SF were added to RCP paste, FA and SF underwent the rehydration in the later stage of cement hydration, which enhanced the pozzolanic effect, thus more CH is consumed.
5. When the content of RCP is not higher than 10%, there is no adverse effect on the pore structure of cement paste. However, when the content of RCP continues to increase, the proportion of harmful pores and more harmful pores of pastes increases, so does the total porosity and most probable pore size. When the paste ratio is F12 (The RCP dosage is 15%, the substitution rate of other mineral admixtures is 15%, FA:SF = 3:2), compared with the control group J0, the proportion of harmless pores increases by 9.672%, the proportion of harmful pores and harmful pores decreases, the pore structure of pastes improves, and the compactness of material structure enhances.

**Acknowledgement:** This research was supported by the National Natural Science Foundation of China (51668052), Qinghai Provincial Science and Technology Department Basic Research Project (2017-ZJ-787) and Qinghai Provincial Science and Technology Department Technology Basic Condition Platform Project (2018- ZJ-T01).

**Funding Statement:** This research was supported by the National Natural Science Foundation of China (51668052), Qinghai Provincial Science and Technology Department Basic Research Project (2017-ZJ-787) and Qinghai Provincial Science and Technology Department Technology Basic Condition Platform Project (2018- ZJ-T01).

**Conflicts of Interest:** The authors declare that they have no conflicts of interest to report regarding the present study.

## References

1. Duan, Z., Hou, S., Xiao, J., Singh, A. (2020). Rheological properties of mortar containing recycled powders from construction and demolition wastes. *Construction and Building Materials*, 237, 117622. DOI 10.1016/j.conbuildmat.2019.117622.
2. Zhang, X., Meng, Y., Ren, J. (2013). Analysis on the current situation and development trend of recycled aggregate concrete at home and abroad. *Concrete*, 7, 80–83.
3. Evangelista, L., Guedes, M., De Brito, J., Ferro, A. C., Pereira, M. F. (2015). Physical, chemical and mineralogical properties of fine recycled aggregates made from concrete waste. *Construction and Building Materials*, 86, 178–188. DOI 10.1016/j.conbuildmat.2015.03.112.
4. Alexandre Bogas, J., De Brito, J., Ramos, D. (2016). Freeze-thaw resistance of concrete produced with fine recycled concrete aggregates. *Journal of Cleaner Production*, 115, 294–306. DOI 10.1016/j.jclepro.2015.12.065.
5. Xiao, J., Ma, Z., Sui, T., Akbarnezhad, A., Duan, Z. (2018). Mechanical properties of concrete mixed with recycled powder produced from construction and demolish waste. *Journal of Cleaner Production*, 188, 720–731. DOI 10.1016/j.jclepro.2018.03.277.
6. Bordy, A., Younsi, A., Aggoun, S., Fiorio, B. (2017). Cement substitution by a recycled cement paste fine: Role of the residual anhydrous clinker. *Construction and Building Materials*, 132, 1–8. DOI 10.1016/j.conbuildmat.2016.11.080.
7. Leteliera, V., Henriquez-Jara, B. I., Manosalva, M., Moriconi, G. (2019). Combined use of waste concrete and glass as a replacement for mortar raw materials. *Waste Management*, 94, 107–119. DOI 10.1016/j.wasman.2019.05.041.
8. Braga, M., Brito, J. D., Veiga, R. (2012). Incorporation of fine concrete aggregates in mortars. *Construction and Building Materials*, 36, 960–968. DOI 10.1016/j.conbuildmat.2012.06.031.
9. Puthussery, J. V., Kumar, R., Garg, A. (2016). Evaluation of recycled concrete aggregates for their suitability in construction activities: An experimental study. *Waste Management*, 60, 270–276. DOI 10.1016/j.wasman.2016.06.008.
10. Liu, Q., Tong, T., Liu, S., Yang, D., Yu, Q. (2014). Investigation of using hybrid recycled powder from demolished concrete solids and clay bricks as a pozzolanic supplement for cement. *Construction and Building Materials*, 73, 754–763. DOI 10.1016/j.conbuildmat.2014.09.066.
11. Han, X., Yang, J., Feng, J., Zhou, C., Wang, X. (2019). Research on hydration mechanism of ultrafine fly ash and cement composite. *Construction and Building Materials*, 227, 116697.1–116697.13. DOI 10.1016/j.conbuildmat.2019.116697.
12. Juan-Valdes, A., Rodriguez-Robles, D., Garcia-Gonzalez, J., Ignacio Guerra-Romero, M., Julia, M. D. P. (2018). Mechanical and microstructural characterization of non-structural precast concrete made with recycled mixed ceramic aggregates from construction and demolition wastes. *Journal of Cleaner Production*, 180, 482–493. DOI 10.1016/j.jclepro.2018.01.191.
13. Walid, A. K., Muhammad, N., Megat, A. M. J., Saiful, I. A. B. M., Abdullah, M. et al. (2018). An overview and experimental study on hybrid binders containing date palm ash, fly ash, opc and activator composites. *Construction and Building Materials*, 159(9), 567–577. DOI 10.1016/j.conbuildmat.2017.11.017.

14. Yang, K., Jung, Y., Cho, M. S., Tae, S. H. (2015). Effect of supplementary cementitious materials on reduction of CO<sub>2</sub> emissions from concrete. *Journal of Cleaner Production*, 103(9), 774–783. DOI 10.1016/j.jclepro.2014.03.018.
15. Kim, Y. J., Choi, Y. W. (2012). Utilization of waste concrete powder as a substitution material for cement. *Construction and Building Materials*, 30(2), 500–504. DOI 10.1016/j.conbuildmat.2011.11.042.
16. Sucic, A., Loffy, A. (2016). Effect of new paste volume on performance of structural concrete using coarse and granular recycled concrete aggregate of controlled quality. *Construction and Building Materials*, 108, 119–128. DOI 10.1016/j.conbuildmat.2015.10.064.
17. Moon, D. J., Kim, Y. B., Ryou, J. (2008). An approach for the recycling of waste concrete powder as cementitious materials. *Journal of Ceramic Processing Research*, 9(3), 278–281.
18. Jaroslav, T., Zdenek, P. (2017). Properties and microstructure of cement paste including recycled concrete powder. *Acta Polytechnica*, 57(1), 49–57.
19. Kasami, H., Hosino, M., Arasima, T., Tateyasiki, H. (2001). Use of recycled concrete powder in self-compacting concrete. *Special Publication*, 200, 381–398.
20. Singh, A., Arora, S., Sharma, V., Bhardwaj, B. (2019). Workability retention and strength development of self-compacting recycled aggregate concrete using ultrafine recycled powders and silica fume. *Practice Periodical of Hazardous, Toxic, and Radioactive Waste Management*, 23(4), 04019016.1–04019016.11.
21. Kwon, E., Ahn, J., Cho, B., Park, D. (2015). A study on development of recycled cement made from waste cementitious powder. *Construction and Building Materials*, 83(9), 174–180. DOI 10.1016/j.conbuildmat.2015.02.086.
22. Rangel, C. S., Toledo Filho, R. D., Amario, M., Pepe, M., Gabriela, D. C. P. et al. (2018). Generalized quality control parameter for heterogenous recycled concrete aggregates: A pilot scale case study. *Journal of Cleaner Production*, 208(3), 589–601. DOI 10.1016/j.jclepro.2018.10.110.
23. Chen, X., Li, Q., Qin, Y. (2010). Experimentation and research on concrete crash dust utilization in mortar. *Construction Science and Technology*, 3, 53–55.
24. Sun, Y., Guo, Y., Sun, K., Li, Q. (2011). Experimental study on the recycled powder preparation auxiliary gelled material. *Low Temperature Architecture Technology*, 33(4), 8–10.
25. Ma, Z., Li, W., Wu, H., Cao, C. (2019). Chloride permeability of concrete mixed with activity recycled powder obtained from C&D waste. *Construction and Building Materials*, 199, 652–663. DOI 10.1016/j.conbuildmat.2018.12.065.
26. Liu, Q., Li, B., Xiao, J., Singh, A. (2020). Utilization potential of aerated concrete block powder and clay brick powder from C&D waste. *Construction and Building Materials*, 238, 117721. DOI 10.1016/j.conbuildmat.2019.117721.
27. Edwin, R. S., Gruyaert, E., De Belie, N. (2017). Influence of intensive vacuum mixing and heat treatment on compressive strength and microstructure of reactive powder concrete incorporating secondary copper slag as supplementary cementitious material. *Construction and Building Materials*, 155, 400–412. DOI 10.1016/j.conbuildmat.2017.08.036.
28. Pradhan, S., Kumar, S., Barai, S. V. (2020). Multi-scale characterisation of recycled aggregate concrete and prediction of its performance. *Construction and Building Materials*, 106, 103480.
29. Al-Bayati, H. K. A., Das, P. K., Tighe, S. L., Baaj, H. (2016). Evaluation of various treatment methods for enhancing the physical and morphological properties of coarse recycled concrete aggregate. *Construction and Building Materials*, 112(6), 284–298. DOI 10.1016/j.conbuildmat.2016.02.176.
30. Li, L., Zhang, H., Guo, X., Zhou, X., Lu, L. et al. (2019). Pore structure evolution and strength development of hardened cement paste with super low water-to-cement ratios. *Construction and Building Materials*, 227, 117108.1–117108.13.
31. Zhu, C., Fang, Y., Wei, H. (2018). Carbonation-cementation of recycled hardened cement paste powder. *Construction and Building Materials*, 192(2017), 224–232. DOI 10.1016/j.conbuildmat.2018.10.113.
32. Sun, Z., Liu, F., Tong, T., Qi, C., Yu, Q. (2017). Hydration of concrete containing hybrid recycled demolition powders. *Journal of Materials in Civil Engineering*, 29, 1–7.

33. Bogas, J. A., Carriço, A., Pereira, M. F. C. (2019). Mechanical characterization of thermal activated low-carbon recycled cement mortars. *Journal of Cleaner Production*, 218, 377–389. DOI 10.1016/j.jclepro.2019.01.325.
34. GB/T 1346-2001 (2001). Standard consistency water consumption, setting time and stability test method of cement. China.
35. GB/T 2419-2005 (2005). Method for determination of fluidity of cement mortar. China.
36. GB/T 17671-1999 (1999). Test method for strength of cement mortar (ISO method). China.
37. Duan, Z., Hou, S., Xiao, J., Li, B. (2019). Study on the essential properties of recycled powders from construction and demolition waste. *Journal of Cleaner Production*, 253, 119865. DOI 10.1016/j.jclepro.2019.119865.
38. Alnahhal, M. F., Alengaram, U. J., Jumaat, M. Z., Abutaha, F., Alqedra, M. A. et al. (2018). Assessment on engineering properties and CO<sub>2</sub> emissions of recycled aggregate concrete incorporating waste products as supplements to portland cement. *Journal of Cleaner Production*, 203(10), 822–835. DOI 10.1016/j.jclepro.2018.08.292.
39. Yang, T., Zhu, H., Zhang, Z., Gao, X., Zhang, C. et al. (2018). Effect of fly ash microsphere on the rheology and microstructure of alkali-activated fly ash/slag pastes. *Cement and Concrete Research*, 109, 198–207. DOI 10.1016/j.cemconres.2018.04.008.
40. Moghaddam, F., Sirivivatnanon, V., Vessalas, K. (2019). The effect of fly ash fineness on heat of hydration, microstructure, flow and compressive strength of blended cement pastes. *Case Studies in Construction Materials*, 10(9), e00218. DOI 10.1016/j.cscm.2019.e00218.
41. Shi, C., Li, Y., Zhang, J., Li, W., Chong, L. et al. (2016). Performance enhancement of recycled concrete aggregate—A review. *Journal of Cleaner Production*, 112(2), 466–472. DOI 10.1016/j.jclepro.2015.08.057.
42. Prosek, Z., Nezerka, V., Hluzek, R., Trejbal, J., Tesarek, P. et al. (2019). Role of lime, fly ash, and slag in cement pastes containing recycled concrete fines. *Construction and Building Materials*, 201(9), 702–714. DOI 10.1016/j.conbuildmat.2018.12.227.
43. Cuenca-Moyano, G. M., Martín-Pascual, J., Martín-Morales, M., Valverde-Palacios, I., Zamorano, M. (2020). Effects of water to cement ratio, recycled fine aggregate and air entraining/plasticizer admixture on masonry mortar properties. *Construction and Building Materials*, 230(5), 116929. DOI 10.1016/j.conbuildmat.2019.116929.
44. Jiang, D., Li, X., Lv, Y., Zhou, M., He, C. et al. (2020). Utilization of limestone powder and fly ash in blended cement: Rheology, strength and hydration characteristics. *Construction and Building Materials*, 232(5), 117228. DOI 10.1016/j.conbuildmat.2019.117228.
45. Li, S., Gao, J., Li, Q., Zhao, X. (2021). Investigation of using recycled powder from the preparation of recycled aggregate as a supplementary cementitious material. *Construction and Building Materials*, 267(4), 120976. DOI 10.1016/j.conbuildmat.2020.120976.
46. Ma, J., Yu, Z., Ni, C., Shi, H., Shen, X. (2019). Effects of limestone powder on the hydration and microstructure development of calcium sulphoaluminate cement under long-term curing. *Construction and Building Materials*, 199(9), 688–695. DOI 10.1016/j.conbuildmat.2018.12.054.
47. de Matos, P. R., Prudêncio, L. R., Jr, Pilar, R., Gleize, P. J. P., Pelisser, F. (2020). Use of recycled water from mixer truck wash in concrete: Effect on the hydration, fresh and hardened properties. *Construction and Building Materials*, 230, 116981. DOI 10.1016/j.conbuildmat.2019.116981.
48. Tang, Q., Ma, Z., Wu, H., Wang, W. (2020). The utilization of eco-friendly recycled powder from concrete and brick waste in new concrete: A critical review. *Cement and Concrete Composites*, 114(4), 103807. DOI 10.1016/j.cemconcomp.2020.103807.
49. Han, J., Wang, K., Shi, J., Wang, Y. (2014). Influence of sodium aluminate on cement hydration and concrete properties. *Construction and Building Materials*, 64(11), 342–349. DOI 10.1016/j.conbuildmat.2014.04.089.
50. Mukharjee, B. B., Muduli, R. (2019). Performance assessment of concrete incorporating recycled coarse aggregates and metakaolin: A systematic approach. *Construction and Building Materials*, 233, 117223.
51. Wang, Y., Shui, Z., Gao, X., Huang, Y., Yu, R. et al. (2019). Utilizing coral waste and metakaolin to produce eco-friendly marine mortar: Hydration, mechanical properties and durability. *Journal of Cleaner Production*, 219(12), 763–774. DOI 10.1016/j.jclepro.2019.02.147.

52. Zhang, H., Ji, T., Liu, H. (2019). Performance evolution of the Interfacial Transition Zone (ITZ) in recycled aggregate concrete under external sulfate attacks and dry-wet cycling. *Construction and Building Materials*, 229(5), 116938. DOI 10.1016/j.conbuildmat.2019.116938.
53. Liu, G., Florea, M. V. A., Brouwers, H. J. H. (2019). Characterization and performance of high volume recycled waste glass and ground granulated blast furnace slag or fly ash blended mortars. *Journal of Cleaner Production*, 235, 461–472. DOI 10.1016/j.jclepro.2019.06.334.
54. Ferreira, R. L. S., Anjos, M. A. S., Nobrega, A. K. C., Pereira, J. E. S., Ledesma, E. F. (2019). The role of powder content of the recycled aggregates of CDW in the behaviour of rendering mortars. *Construction and Building Materials*, 208(2), 601–612. DOI 10.1016/j.conbuildmat.2019.03.058.
55. Rajhans, P., Chand, G., Kisku, N., Panda, S. K., Nayak, S. (2019). Proposed mix design method for producing sustainable self compacting heat cured recycled aggregate concrete and its microstructural investigation. *Construction and Building Materials*, 218(2), 568–581. DOI 10.1016/j.conbuildmat.2019.05.149.
56. Vaezi, M., Zareei, S. A., Jahadi, M. (2020). Recycled microbial mortar: Effects of bacterial concentration and calcium lactate content. *Construction and Building Materials*, 234, 117349. DOI 10.1016/j.conbuildmat.2019.117349.
57. Omrane, M., Kenai, S., Kadri, E. H., Ait-Mokhtar, A. (2017). Performance and durability of self compacting concrete using recycled concrete aggregates and natural pozzolan. *Journal of Cleaner Production*, 165, 415–430. DOI 10.1016/j.jclepro.2017.07.139.
58. Indukuri, C. S. R., Nerella, R., Madduru, S. R. C. (2019). Effect of graphene oxide on microstructure and strengthened properties of fly ash and silica fume based cement composites. *Construction and Building Materials*, 229(7100). DOI 10.1016/j.conbuildmat.2019.116863.
59. Rais, M. S., Shariq, M., Masood, A., Umar, A., Alam, M. M. (2019). An experimental and analytical investigation into age-dependent strength of fly ash mortar at elevated temperature. *Construction and Building Materials*, 222(4), 300–311. DOI 10.1016/j.conbuildmat.2019.06.167.
60. Kalinowska-Wichrowska, K., Pawluczuk, E., Bołtryk, M. (2019). Waste-free technology for recycling concrete rubble. *Construction and Building Materials*, 234(9), 117407. DOI 10.1016/j.conbuildmat.2019.117407.
61. Harilal, M., Rathish, V. R., Anandkumar, B., George, R. P., Mohammed, M. S. H. S. et al. (2018). High performance green concrete (HPGC) with improved strength and chloride ion penetration resistance by synergistic action of fly ash, nanoparticles and corrosion inhibitor. *Construction and Building Materials*, 198(8), 299–312. DOI 10.1016/j.conbuildmat.2018.11.266.
62. Wu, Z., Lian, H. (1999). *High performance concrete*, pp. 24–25. Beijing: China Railway Publishing House.
63. Florea, M. V. A., Brouwers, H. J. H. (2013). Properties of various size fractions of crushed concrete related to process conditions and re-use. *Cement and Concrete Research*, 52(8), 11–21. DOI 10.1016/j.cemconres.2013.05.005.
64. Zhang, C., Kong, X., Lu, Z., Jansen, D., Pakusch, J. et al. (2018). Pore structure of hardened cement paste containing colloidal polymers with varied glass transition temperature and surface charges. *Cement and Concrete Composites*, 95, 154–168. DOI 10.1016/j.cemconcomp.2018.11.001.
65. Mukharjee, B. B., Muduli, R. (2019). Performance assessment of concrete incorporating recycled coarse aggregates and metakaolin: A systematic approach. *Construction and Building Materials*, 233, 117223.
66. Ogawa, Y., Bui, P. T., Kawai, K., Sato, R. (2020). Effects of porous ceramic roof tile waste aggregate on strength development and carbonation resistance of steam-cured fly ash concrete. *Construction and Building Materials*, 236, 236117462. DOI 10.1016/j.conbuildmat.2019.117462.
67. Yang, J., Wang, L., Jin, C., Sheng, D. (2020). Effect of fly ash on the corrosion resistance of magnesium potassium phosphate cement paste in sulfate solution. *Construction and Building Materials*, 237(4), 117639. DOI 10.1016/j.conbuildmat.2019.117639.
68. Nguyen, H. A., Chang, T. P., Shih, J. Y., Chen, C. T. (2019). Influence of low calcium fly ash on compressive strength and hydration product of low energy super sulfated cement paste. *Cement and Concrete Composites*, 99(12), 40–48. DOI 10.1016/j.cemconcomp.2019.02.019.